Optical emissions and behaviors of the blue starters, blue jets, and gigantic jets observed in the Taiwan transient luminous event ground campaign

J. K. Chou,[1] L. Y. Tsai,[1] C. L. Kuo,[1,2,3] Y. J. Lee,[1] C. M. Chen,[1] A. B. Chen,[4,5] H. T. Su,[1,2] R. R. Hsu,[1,2] P. L. Chang,[6] and L. C. Lee[3]

Received 30 September 2010; revised 24 March 2011; accepted 4 April 2011; published 7 July 2011.

[1] On 22 July 2007, 37 blue jets/starters and 1 gigantic jet occurring over a thunderstorm in the Fujian province of China were observed from the Lulin observatory on the central mountain ridge of Taiwan. The majority of the jets were observed to occur in a 5 min window during the mature phase of the jet-producing thunderstorm. These jets have significant red band emissions. However, the blue emissions from these jets were not discernible due to severe atmospheric scattering. A model estimation of the emissions from a streamer reveals that the red emissions in blue starters and blue jets are mainly from the nitrogen first positive band ($1PN_2$). The type II gigantic jet is the first of this type that was observed from the ground. The generation sequence of the gigantic jet begins with a blue starter, then a blue jet occurs at the same cloud top after ~100 ms and finally develops into a gigantic jet ~50 ms later. Using "optical strokes" as surrogates of the lightning strokes, the correlations between jets and the cloud lightning are explored. The results indicate that the occurrence of jets can be affected by the preceding local cloud-to-ground (CG) lightning or nearby lightning (intracloud (IC) or CG), while in turn the jets might also affect the ensuing lightning activity.

Citation: Chou, J. K., L. Y. Tsai, C. L. Kuo, Y. J. Lee, C. M. Chen, A. B. Chen, H. T. Su, R. R. Hsu, P. L. Chang, and L. C. Lee (2011), Optical emissions and behaviors of the blue starters, blue jets, and gigantic jets observed in the Taiwan transient luminous event ground campaign, *J. Geophys. Res.*, *116*, A07301, doi:10.1029/2010JA016162.

1. Introduction

[2] Jets, a category of transient luminous events (TLEs) [*Pasko*, 2010, and references therein], are upward discharges from thunderstorm tops (~15–18 km). More prominent species of jets including blue starters, blue jets (BJs) [*Wescott et al.*, 1995], and gigantic jets (GJs) [*Pasko et al.*, 2002; *Su et al.*, 2003] are differentiated by their terminal altitudes. Other smaller varieties of upward discharges called "gnomes" and "pixies" have also been observed in ground observations [*Lyons et al.*, 2003]. For convenience, regardless their vertical scales, the variants of electric discharges from cloud tops may be collectively called the electric jets, a term that was first used in the work of *Pasko* [2003]. Using three-color cameras (red: 560–710 nm, green: 470–590 nm, blue: 390–510 nm) during Sprite94 aircraft campaign, blue jets and blue starters occurring over thunderstorms were first observed by *Wescott et al.* [1995, 1996]. The color of the recorded events is primarily blue, and the emissions of the events are mainly from N_2 second positive band ($2PN_2$) [*Wescott et al.*, 1998]. They also concluded that the recorded blue jets and blue starters had no detectable red component due to the strong quenching effect on $1PN_2$ in the low-altitude region.

[3] A typical blue jet has a fountain-like cone shape with plane cone angle of ~15°. Its terminal altitude is about 40–50 km, its upward velocity is ~100 km/s, and the overall luminous duration is about 200–300 ms [*Wescott et al.*, 1995]. The blue starters move upward only a few kilometers with an averaging terminal altitude of 20.8 km [*Wescott et al.*, 1996]. During the EXL 98 sprite aircraft campaign, a low-light level camera equipped with a narrow 427.8 nm band filter was deployed to detect the N_2^+ first negative band emissions ($1NN_2^+$) [*Wescott et al.*, 2001]. They found that the ionized N_2 emission band contributes only 3% toward the recorded blue light and concluded that the blue starters are partially ionized.

[4] Gigantic jets, the largest forms of upward discharges from cloud tops, develop to the lower ionosphere (~70–90 km altitude) and have been observed from ground and space [*Pasko et al.*, 2002; *Su et al.*, 2003; *van der Velde et al.*, 2007; *Kuo et al.*, 2009; *Cummer et al.*, 2009]. From analyses of the

[1]Department of Physics, National Cheng Kung University, Tainan, Taiwan.
[2]Earth Dynamic System Research Center, National Cheng Kung University, Tainan, Taiwan.
[3]Institute of Space Science, National Central University, Jhongli, Taiwan.
[4]Institute of Space, Astrophysical and Plasma Sciences, National Cheng Kung University, Tainan, Taiwan.
[5]Plasma and Space Science Center, National Cheng Kung University, Tainan, Taiwan.
[6]Central Weather Bureau, Taipei, Taiwan.

0148-0227/11/2010JA016162

GJ events recorded by Imager of Sprites and Upper Atmospheric Lightning (ISUAL), a payload of the FORMOSAT-2 satellite, gigantic jets can be categorized into three types from their dynamic morphology [*Chou et al.*, 2010]. The morphological evolution of the type I GJs is similar to those observed from the ground and consists of three stages, the leading jet (LJ), the fully developed jet (FDJ), and the trailing jet (TJ) with a combined luminous duration of 500 ms or greater [*Su et al.*, 2003]. Type I GJs are discharges from cloud to the ionosphere with negative streamer polarity (−CI), a classification supported by clear associated ELF signals [*Su et al.*, 2003; *Cummer et al.*, 2009]. The type I GJs observed by *Su et al.* [2003] showed a leading jet lasting 1–2 NTSC image fields (one field is ~17 ms) and then developed into a fully developed jet that stayed luminous for 2–5 image fields for the cases of tree-like GJs and 10–16 image fields for the carrot-like GJs. After completing the discharge channel to the ionosphere, the trailing jet of the type I GJs persists for 13–21 image fields. Using high-resolution ISUAL spectroscopic data, *Kuo et al.* [2009] deduced the altitudinal variation of the reduced electric field (400–655 Td) and the average electron energy (8.5–12.3 eV) in the type I GJs. They also suggested that the FDJ stage contains ionized discharge channel that lowered the local ionosphere boundary to ~50 km and then a return-stroke-like process would occur from that altitude and develops toward the cloud top. The continuous current flows along this conducting channel and its contact point with the local ionosphere boundary moves upwardly due to the attachment process forming the observed upward surging trailing jets. The type II GJ begins as a blue jet and then the upward discharge develops further to reach the lower ionosphere. Because of the dimmer brightness of the FDJ streamers in the type II GJs compared with type I GJs, the smaller minimum field needed to propagate positive streamers, and a probable type II GJ with clear ULF detection, it is believed that the type II GJs are positive discharges from cloud to the ionosphere (+CI) [*Chou et al.*, 2010]. Type III GJs are closely preceded by lightning and have brightness that ranges between that for the type Is and the type IIs. The discharge polarity of the type III GJs is expected to be either positive or negative depending on the charge imbalance left behind by the preceding lightning [*Chou et al.*, 2010]. A comparison of the characteristics for the three types of GJs can be found in Table 2 of *Chou et al.* [2010].

[5] If jets are upward discharging counterparts of the cloud-to-ground lightning, the interplay between jets and lightning is an interesting subject and has indeed been explored before. Using the NLDN cloud-to-ground (CG) lightning data, *Wescott et al.* [1996] reported that within a radius of 50 km area, a sudden reduction of −CGs persisted about 3 s after the occurrence of blue starters. They speculated that the occurrence of −CG flashes before the jet is possibly a factor in priming the cloud charge configuration that leads to the jet initiation. After the occurrence of blue jets/starters, the energy of thundercloud decreased and led to the reduction in the −CGs' occurrence rate. Similar correlation pattern between blue jets and lightning was also found for the area within 15 km of the blue jets [*Wescott et al.*, 1998].

[6] From these correlation patterns and the observed streamer structure of BJs, *Pasko et al.* [1996] and *Pasko and George* [2002] modeled blue jets as the upward positive streamer discharges from cloud top for a given charge distribution in the thundercloud. *Petrov and Petrova* [1999] originally proposed that BJs are the streamer zones of the positive leaders. *Raizer et al.* [2006, 2007] further proposed that a blue jet consists of an upward propagating leader to sustain the long duration discharge and the "trunk" on the base of the jets shown in the photographs might be the manifestation of leaders. *Krehbiel et al.* [2008] proposed a unified model for all the thundercloud discharges. They conjectured that in the normally electrified thunderstorms, the blue jets initiate between the upper positive charge layer and the screen charge layer on the top of the cloud, following the occurrence of −CGs that changed the electric field in the cloud. Gigantic jets originate from the midlevel negative charge layer and propagate upward to the lower ionosphere. Recently, *Riousset et al.* [2010] quantitatively modeled the mixing effect on the initiation of the blue jets. They proposed that the accumulation of the upper screen charge layer near the cloud boundary leads to the initiation of blue jets, while the strong mixing of these charge with the upper thundercloud charge may lead to the formation of gigantic jets.

[7] In this paper we report detailed analyses of the 38 jets recorded on 22 July 2007 over a thunderstorm in the Fujian province of China. One of them is a type II gigantic jet which was the first GJ of this type that was recorded from the ground. The images reported in this work were recorded by a cluster of filter-equipped cameras. The jets are found to have significant red emissions and its implication will be discussed. Since no lightning-associated sferics from this thunderstorm during the jet-generating period were found, correlation patterns between the jets and the lightning activity are analyzed based on the illumination of cloud from ICs and CGs. The correlation patterns show considerable complexity and can be categorized into four types. The interpretation of lightning and jets interactions based on these correlation patterns will be discussed in detail.

2. Observational Data

[8] During 12:18~14:35 UTC on 22 July 2007, a thunderstorm extending over Fujian province of China was tracked from Lulin observatory (120°52′25″E, 23°28′07″N; 2862 m elevation) in Taiwan. Three sight-aligned WATEC 100-N cameras were deployed to simultaneously monitor the storm cells forming along the outflow boundary of a small mesoscale convective system (MCSs; Figure 1a) [*Knupp et al.*, 1998] at the standard NTSC frame rate (30 frames/s or 60 image fields/s). The responsive curve of the WATEC 100-N CCD contains a maximum at 620 nm, and the sensitivity drops down to half of the peak value at 400 nm and 775 nm. A camera, which was equipped with an 8 mm/f1.2 lens, no filter, and has a field of view (FOV) of 46.2°H × 34.7°V, was used as the finder for the observation. The other two cameras are equipped with 12 mm/f1.2 lenses (FOV: 30.8°H × 23.1°V) and either red band filter (effective passing band: 540 ~ 1000 nm) or blue band filter (effective passing band: 340 ~ 540 nm). For this observation, the CCD gain of the red band camera was set at 20% that of the blue-camera to prevent the images from saturating. Using the star

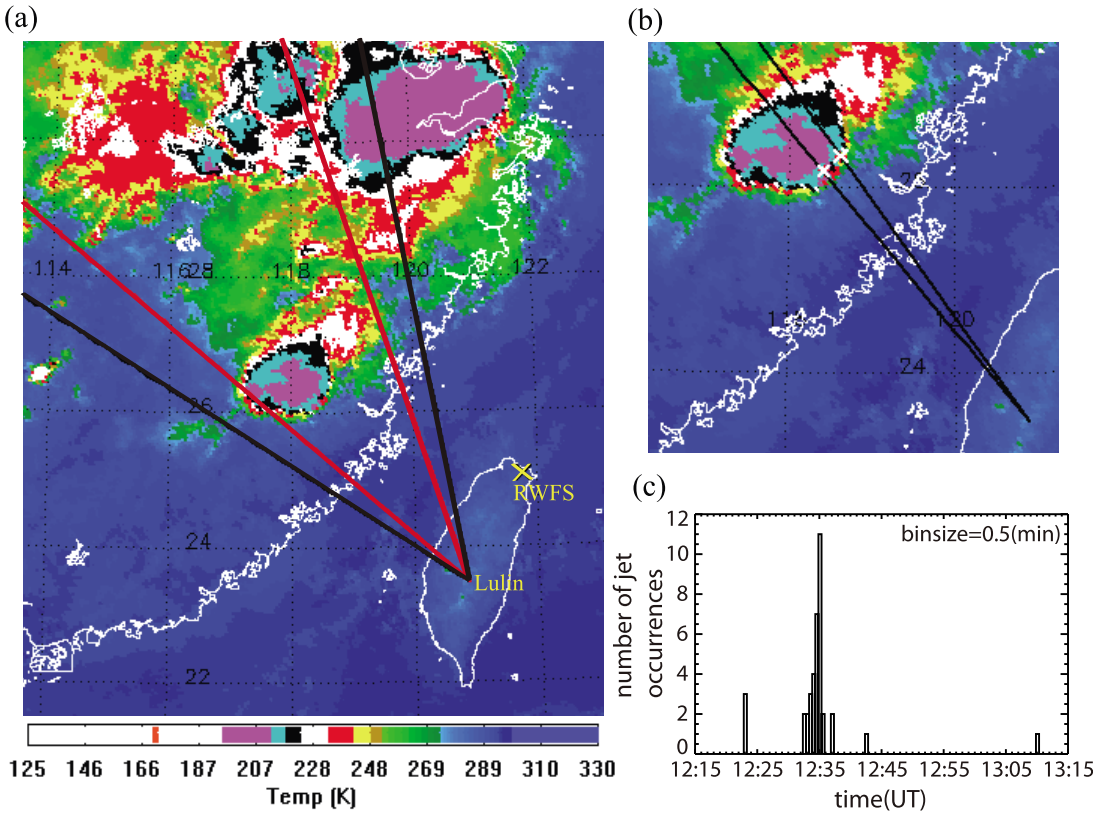

Figure 1. (a) MTSAT infrared cloud map at 22 July 2007, 13:00 UTC. The two red lines denote the field of view (FOV) of the red and the blue cameras. The two black lines represent the wider FOV of the unfiltered finder camera. Five sprites were observed from a mesoscale convective system (MCS) about 750 km north of the Lulin observatory (120°52′25″E, 23°28′07″N). All jets and three additional sprites occurred over the smaller thunderstorm 400 km northwest of the observatory. (b) The zoom-in view of the thunderstorm in Figure 1a. The observed jets distributed along the two black lines, and the line-of-sight scatters for each group are less than the line width. The two white crosses mark the regions having the maximum radar reflectivity in the two convective cells during the jet occurring period (see Figure 2). The two crosses are on the lines of sight for the two groups of jets, and they are assumed to be the emerging regions of the jets. (c) Temporal occurring histogram of the jets. The color palette under Figure 1a denotes the cloud top temperatures of this region at 22 July 2007 13:00 UTC. RWFS is the code name for the Wu-Fen-Shan radar station.

field as the guide, the elevation angle is found to be 10° and the azimuth angle is 327° for the FOV center.

[9] For the duration of the observation, 38 jets (37 blue jets/starters and a gigantic jet) and 8 sprites were recorded. Five sprites were from a MCS about 750 km north of Lulin observatory (Figure 1a). All the jets and the three additional sprites are from a smaller, 100 km diameter thunderstorm that located about 400 km northwest of the Lulin Observatory. The three sprites appeared about 80 min later than the jets. The azimuths of the observed jets are actually clustering into two distinct groups and are denoted by the two black lines in Figure 1b. The azimuth spread of the jets in each group is smaller than the line width. Figure 1c presents the temporal histogram for the jets occurrence. A short burst of 33 blue jets/starters occurs in a 5 min window around 12:35 UTC, during the mature phase of the jet-producing thunderstorm.

[10] The life cycle of the jet-producing thunderstorm is about 4 h between 10:30 UTC and 14:30 UTC, as estimated from the reflectivity observations of the Wu-Fen-Shan radar station (RCWF; 121°46′22″E, 25°04′22″N; 766 m elevation). This thunderstorm reached its maximum reflected intensity at 11:50 UTC with a reflectivity of ~53.0 dBZ. Figure 2 shows the radar reflectivity of this storm respectively at 12:00, 12:30, and 13:00 UTC. At 12:00 UTC, the W01 convective cell was detected to have the maximum reflectivity of ~52 dBZ (Figure 2a). After the W01 cell weakened, the W02 cell intensified and showed a maximum reflectivity of ~44 dBZ at 12:30 UTC (Figure 2b). At 13:00 UTC, the thunderstorm showed the signatures of weakening reflectivity with a significant anvil (Figure 2c); hence it is presumed that the lifetime of the thunderstorm was in the mature to the dissipating stages.

[11] The jet-producing storm was located at the effective probing edge of the RCWF station (~360 km distance). Only the first two low-elevation scans (0.5° and 1.5°) produced analyzable reflectivity. Since the convective cells were captured by the second 1.5° elevation scan of the RCWF radar and their reflectivity was greater than 18.5 dBZ, the echo tops can presumably be used to infer the vertical extent of the convective cells [*Amburn and Wolf*, 1997]. However, owing to the low elevation and the remoteness of the radar scan, the

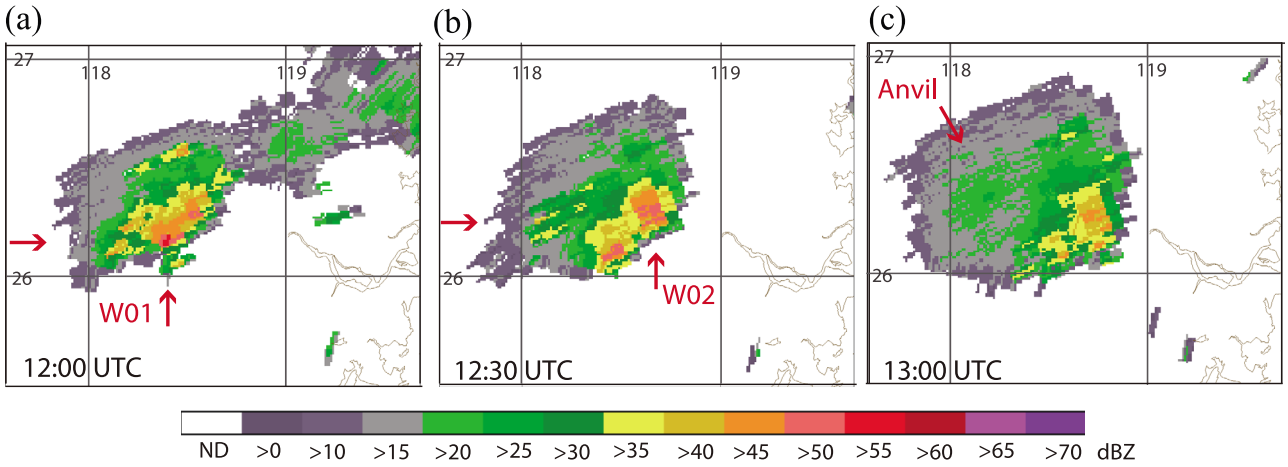

Figure 2. Radar reflectivity maps of the jet-producing thunderstorm at (a) 12:00, (b) 12:30, and (c) 13:00 UTC, 22 July 2007. Figure 2a shows that the convective cell W01 has a maximum radar reflectivity of 52 dBZ at 12:00 UTC. Figure 2b shows that the convective cell W02 has a maximum radar reflectivity of 44 dBZ at 12:30 UTC. The maximum reflectivity was captured by the second tilt (1.5°) of the RCWF radar for both W01 and W02 cells. The base, the centerline, and the top of the radar beam height are ~14, ~17, and ~20 km at a range ~360 km. Figure 2c shows that the thunderstorm shows a weakening reflectivity and has developed an extended anvil region at 13:00 UTC, which signifies that it is in the mature to the dissipating stage.

radio beam suffers more broadening. The base, the centerline, and the top of the radar beam heights for this tilt are ~14, ~17, and ~20 km at a range of ~360 km. As a result, the echo tops, and hence the cell tops, could be presumed to be above 14 km from the lower bound of the beam height.

[12] Besides using the radar data to infer the lower bound altitude of the cloud tops, additional constraints can be obtained from the brightness temperature of the satellite infrared cloud map and the radiosonde data (Fuzhou station; data were retrieved from http://weather.uwyo.edu/upperair/seasia.html). The brightness temperatures were −65.9°C for the W01 cell and −58.5°C for the W02 cell on the closest available Multifunctional Transport Satellite (MTSAT) infrared map at 13:00 UTC. With the local radiosonde profile obtained at 12:00 UTC, the corresponding cloud heights are inferred to be ~14.1 km (W01 cell) and ~13.4 km (W02 cell). However, at 13:00 UTC, the thunderstorm has entered the decaying phase; thus the updraft motion is expected to subside considerably. Hence the cloud top heights of the two convective cells at 13:00 UTC should be lower than those at the times (~12:30 UTC) when most of the jets occurred but can still serve as a lower bound for the cell top height at 12:30 UTC. In Figure 1b the maximum radar reflectivity regions for the two convective cells are marked by the white crosses. The two regions locate along the azimuthal directions of the jets. Therefore the observed jets are most likely emerging from these two protruding cloud top regions. After taking the curvature of the Earth into account [*Hsu et al.*, 2003], the distances of the protruding tops and the jets are inferred to be ~390 km and the bases of the jets are 15.5 km in altitude. After combining the cell top heights inferred from the radar echo, the infrared cloud temperature, and the optical observation, the heights of the 15 km for the two convective cells at the jet occurring period are reasonable values.

[13] In the past 2 decades, compared with the red sprites, only a few blue jets/starters have been reported in all the TLE ground campaigns around the globe. A plausible reason for the scant ground sighting of blue jets/starters may lie in their relative low terminal altitudes, which render them be easily blocked by the shielding clouds if the occurrence locations are not near the outlying regions. As shown in Figure 2, the active jet-producing regions of this thunderstorm are at the near edge facing the Lulin Observatory. Hence the unusually favorable placement of the jet-producing regions in this thunderstorm may have been a primary factor that contributes to the observation of these blue jets/starters.

3. The First Type II Gigantic Jet Recorded on the Ground

[14] Amidst the jets, at 12:22:50 UTC, a blue starter occurred over the W01 convective cell (Figure 2a). After about 100 ms a blue jet appeared near the same cloud top region and then developed into a gigantic jet 50 ms later (Figure 3). This gigantic jet reached at least ~65 km in elevation, while the emissions above these altitudes were blocked by the clouds near the observatory. It is the first type II GJ [*Chou et al.*, 2010, Figure 2] ever been recorded from the ground. Beside another blue starter occurred over the W01 cell at 12:42:51 UTC, all the remaining blue jets/starters occurred over the W02 cell.

[15] The recorded images indicate that after this type II GJ discharge reaches the ionosphere, then a trailing-jet-like luminous column rises up from the cloud top to ~35 km and lasts for less than 17 ms (one image field). This feature is consistent with the luminous evolution of the type II GJs observed in the ISUAL experiment [*Chou et al.*, 2010]. The persisting time of the trailing luminous column in a type II GJ is far shorter than the 180 ms or greater for the typical

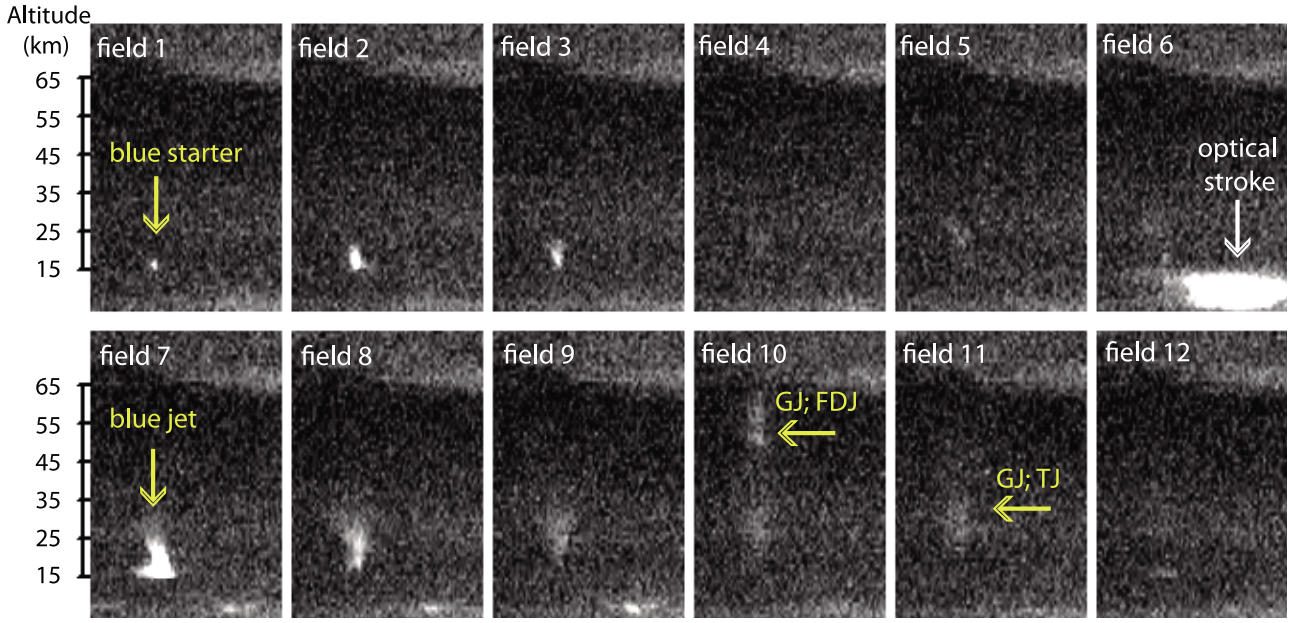

Figure 3. Image sequence (cropped and enhanced) of the type II gigantic jet (GJ) at 12:22:50 UTC from the unfiltered camera. A blue starter (12:22:50.607 UTC) occurs in field 1 and extends upward to ~25 km altitude. Then a blue jet (12:22:50.707 UTC) occurs in field 7 at the same location and finally develops into a gigantic jet (12:22:50.707 UTC) in field 10. At the fully developed jet stage of this type II GJ, its discharge channel connects the cloud top and the ionosphere. A trailing-jet-like luminous column rises up to ~35 km in field 11, following the FDJ. The camera FOV is veiled by thin clouds. Hence, a part of the upper luminous body of this GJ is blocked.

trailing jet of the type I GJs [*Kuo et al.*, 2009]. It may be that even this type II GJ is able to complete the discharge channel to the ionosphere, but the ensuing continuous current from the cloud top is substantially weaker than that in the type I GJs. If one takes the evolution of the type I GJs recorded by *Su et al.* [2003] as the templates, the preceding blue jet for the type II GJ reported in this work may have served as the leading phase of the ensuing gigantic jet. In this sense, most of the blue starters or blue jets maybe are upward discharges that fail to establish discharge channels to the ionosphere.

[16] We had searched for the associated ELF (extremely low frequency, 1–100 Hz) sferics of this GJ in the data set recorded at the Syowa station (69.018°S, 39.506°E), Antarctica [e.g., *Sato and Fukunishi*, 2003]. However, no clear and conclusive signal was found, in line with the situation of the ISUAL type II GJs studied by *Chou et al.* [2010].

[17] During the decaying phase of the jet-producing thunderstorm, as indicated by the obvious anvil structure in the radar reflectivity data shown in Figure 2c, three sprites were observed to occur over this thunderstorm. It is believed that the positive charge layer in the stratiform region of a MCS is an important charge reservoir for +CGs with long-lasting continuous current to induce red sprites [*Lyons*, 1996; *Williams*, 1998; *Lang et al.*, 2010]. On the basis of these previous studies and the model of the MCS electrical structure [*Stolzenburg et al.*, 1994], the electrical structure of the deep convection region in this jet-producing thunderstorm likely is a positive-on-negative tripole. Hence in the following sections, all the discussions are based on the assumption that the jet-producing thunderstorm has a normal electrical structure.

[18] As the preceding blue starter and blue jet depleted the charge in the screening layer, a charge imbalance between the upper positive and the main negative charge layers may favor a −GJ discharge to develop along the channel established by the previous +BJ. Since the luminous emission of the trailing-jet-like column only persists for one image field, it is a good indication that the charge reservoir for this type II GJ is the upper charge layer, which may not have sufficient charge to supply a long-lasting trailing jet. Therefore the type II GJ could be the blue-jet-type discharge that was proposed by *Krehbiel et al.* [2008], whose altitudes could reach ionosphere in an unconstrained potential environment.

4. Jets With Significant Red Emissions

[19] Figures 4a–4c exhibit a set of cropped images recorded by the three cameras for a sprite occurring about 400 km away. Images taken without filter and with red filter both record clear sprite emissions, whereas the sprite emissions in the blue filter image are weak but recognizable after enhancement. Figures 4d–4f contain images from a blue jet with a similar event distance as the sprite shown in Figures 4a–4c. In the red camera image the emissions from the base of this blue jet are clearly visible, but the brightness is much lower than that in the sprite. However, owing to the atmospheric scattering, the blue emissions from this blue jet are not discernible. We use the Moderate Resolution Atmospheric Transmission (MODTRAN) atmospheric code [*Ontar Corporation*, 2002] to estimate the molecular scattering from the jets to observatory. Figure 5 shows the effective response curves of our filter-equipped cameras at the Lulin Observatory to a 15 km altitude emission source

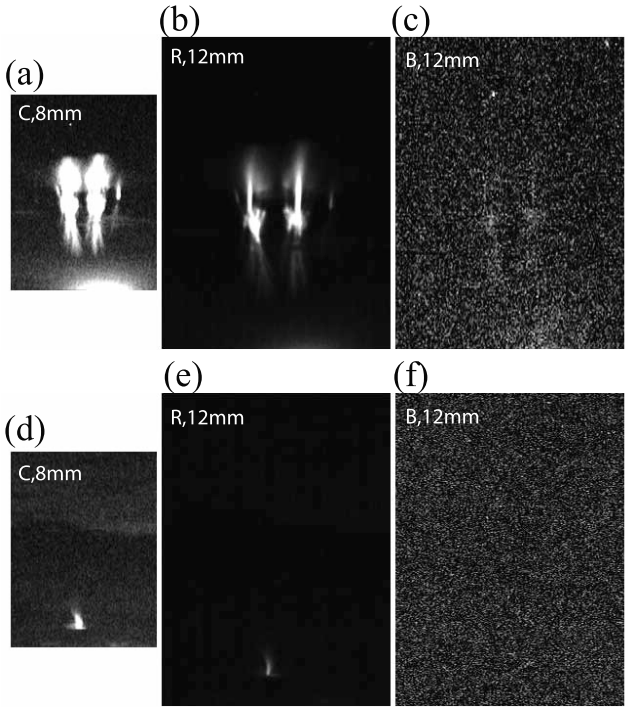

Figure 4. Images (cropped) taken by cameras with (a) no filter, (b) red filter, and (c) blue filter for carrot sprites occurring at 13:52:20 UTC; the blue filter image contains discernible sprite emissions after enhancement. Images taken by cameras with (d) no filter, (e) red filter, and (f) blue filter for a blue jet occurring at 12:22:50 UTC; even after enhancement, the blue emissions from this blue jet failed to stand out.

that locates 400 km away. Note that these effective response curves have taken the atmospheric transmittance, the camera passing band, and the CCD gain setting all into account. For convenience, the major emission lines of nitrogen in the wavelength range of 350–1000 nm are also overlapped.

[20] The main process for streamer discharges in the Earth atmosphere is the collision between electrons and the molecular nitrogen. The main resulting emissions from nitrogen are $1PN_2$ (478–2531 nm), $2PN_2$ (268–546 nm), LBH N_2 (100–240 nm), and $1NN_2^+$ (286–587 nm) [*Kuo*, 2007, Table 3–2]. In Figure 5, the $1PN_2$, $2PN_2$, and $1NN_2^+$ band emissions and their relative intensity are calculated using the method reported by *Kuo et al.* [2008]. It is known that the electric field enhancement around the streamer head can reach ~5 E_k [*Pasko and George*, 2002, and references therein]; E_k is the conventional breakdown threshold in air and is ~32 kV/cm at ground. Under the assumption of a steady state emission [*Kuo et al.*, 2005, equation (2), and references therein], the intensity ratio for emissions recorded by different filter-equipped CCD cameras can be computed. By considering the emissions from nitrogen under a 5 E_k driving electric field and after taking the quenching effect at ~20 km altitude (the blue jet/starter altitude), the atmospheric transmittance, the camera passing band, and the CCD gain setting into account, the intensity ratio between our red band and blue band cameras is estimated to be 2.1 and the intensity ratio between the unfiltered camera and the red band camera comes out to be 6.2. We analyze some of the recorded blue starters/jet events, and find that the brightness ratio for the jets recorded by the unfiltered finder camera and the red-filter camera is ~5, which is close to the theoretical ratio of ~6.

[21] In this ground observation, the red camera has a passing band of 540–1000 nm, which is broader than the red band component (560–710 nm) of the color TV camera deployed in the Sprite94 campaign [*Wescott et al.*, 1995, 1998]. As shown in Figure 5, if blue starters/jets are streamers in nature, the red component would be the $1PN_2$ band emissions. It is also consistent with the ISUAL recorded images of blue starters/jets through a $1PN_2$ band filter [*Chou et al.*, 2010, Figure 3]. The quenching height of the $1PN_2$ band is ~53 km [*Vallance-Jones*, 1974, p. 119]. Hence the red emissions in blue starters and blue jets should be very dim at the low, 15–20 km altitudes. However, owing to the broader passing band in the red camera, more $1PN_2$ emissions can pass through and result in the discernible red band images. Also as exhibited in Figure 5, the blue emissions should be intrinsically dim due to a very low and narrow effective passing band of the blue-filter-equipped camera; even though the blue band camera's gain was set at five times that of the red band camera. Therefore it is not surprising that the blue emissions from jets are buried under noise and cannot be discerned.

5. Lightning Activity in the Jet-Producing Storm

[22] Optical images recorded during the observation period indicate that the clouds in the FOV are constantly illuminated by lightning discharges. Hence lightning data from World Wide Lightning Location Network (WWLLN) [*Rodger et al.*, 2006] was initially used to locate lightning in the observed region. However, it may be that most of the lightning flashes in this area are intracloud or CG lightning with relative weak peak currents, only one WWLLN lightning was found within the 10 s windows of these jets. Therefore we revolve to use the cloud illuminations of the lightning in the recorded images as indicators of the lightning activity.

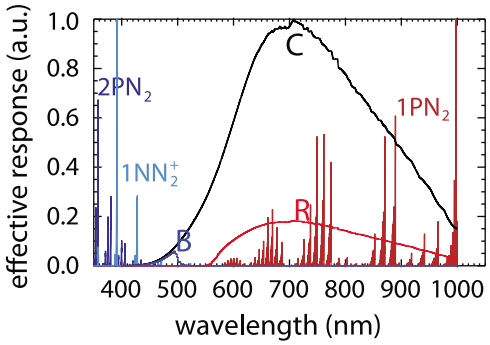

Figure 5. Effective response curves of the three cameras, unfiltered finder camera (C, black curve), red band camera (R, red curve), and blue band camera (B, blue curve). The curves have taken the atmospheric transmittance, the camera passing band, and the CCD gain setting into account. The major spectral lines and the relative intensity of the $1PN_2$, $2PN_2$, and $1NN_2^+$ bands are also shown.

[23] The elevation angle of the cloud top where the jets emerge is 0.10° ± 0.07°, and the elevation angle of the base of the most intense lightning is −1.34° ± 0.07°. Since the event distance is ~390 km and the Lulin site has a nearside view of the jet-producing thunderstorm, this angular spacing corresponds to a vertical separation of ~10 km, which roughly is the vertical extension of the cloud. Moreover, viewing from a single site, the line-of-sight distance of the lightning event cannot be resolved. Only its lateral distance on the image can be determined with sufficient accuracy. From Figure 2b the jet-producing convective cells are at the edge of the thunderstorm facing the observatory, and its size along the line of sight is less than 20 km. Therefore we only consider the azimuthal distance between the jets and the lightning as the major factor contributing to the interaction of lightning and jets.

[24] To avoid bright lightning from saturating the low-light level CCD and hindering the determination of the lightning azimuth, the images from the gain-reduced red camera are chosen for this analysis. To locate lightning on the image frames, we use a tree-search method to find the pixels whose brightness exceeds 10 standard deviations of the mean image brightness in an image field. If more than 10 standout pixels are connected to each other, it is defined as a "bright cluster." Since the vertical span of a bright cluster provides no useful distance information, we sum the image intensity count for all the pixels in a vertical column of a bright cluster. The column possessing the highest intensity counts is taken to be the azimuthal center of the bright cluster. The horizontal extend of the bright cluster is defined as the azimuthal size. The horizontal full width at half maximum (FWHM) width of a bright cluster is used to denote the FWHM azimuthal size of a bright cluster on the image. When the azimuth center of a bright cluster is within the FWHM azimuth size of the previous cluster, they belong to the same lightning activity sequence.

[25] A bright cluster, which brightness and/or area are greater than those on the previous and the following image frames in the same lightning activity sequence, counts as an "optical stroke" (for an example, see the field 6 in Figure 3). For a lightning stroke, the intensity level of the visible flash goes through an intensifying, peaking, and diming cycle. Since the average interval between strokes of CG lightning is 60 ms or greater [*Rakov and Uman*, 2003, p. 7, Table 1.1; p.222] and the exposure time of an image field for the NTSC cameras is 16.68 ms (the uncertainty should be less than 1 ms), optical strokes can provide good facsimile representation of lightning strokes. Hence by defining an optical stroke this way, it is a faithful surrogate of a lightning stroke. Therefore by analyzing the activity of the optical strokes before and after a jet, the interplay between the lightning and the jets can be studied.

[26] We select lightning whose lateral displacement in relative to the jets is less than 50 km and count the number of optical strokes occurring within 10 s window of the jets, following the convention adapted by *Wescott et al.* [1996, 1998]. The cumulative distributions of optical strokes within 50 km lateral distance and within 10 s window of all the observed jets are analyzed. The representation patterns are shown in Figure 6 (left). The vertical red lines denote the relative occurring time of the jets.

[27] Figure 6 (right) shows the accompanying graphs for the sequence of lightning-jet events depicted in Figure 6 (left), and their aim is to provide additional physical information including the temporal evolution (abscissa), the spatial variation (ordinate), the lateral span (gray line), FWHM of the lateral span (red line), and the brightness (color of the dot; the color palette is located under Figure 6h) of the optical strokes occurring within 5 s window of a targeted jet event.

6. Correlation Patterns Between Jets and Lightning

[28] From the optical stroke (lightning)-jet correlation patterns, important information on the interplay of the lightning and jets can be inferred. From analyzing the observed events, four representative patterns for the optical strokes occurring around the jets are found. The salient features of the optical stroke patterns are as follows:

[29] 1. Lightning activity increases before the jets and pauses after for a short period (13 events). As indicated in Figure 6a, two blue starters occurred almost consecutively near t = 0 ms. The cumulative optical stroke pattern indicates that the occurrence of optical strokes intensifies within 0.5 s prior the blue starters, and then falls silent for 0.5 s after. This lightning-jet correlation pattern is similar to the lightning flash pattern reported by *Wescott et al.* [1996, 1998]. In Figure 6b the vertical blue dashed lines denote the relative occurrence time of two blue starters. The crosses on the vertical dashed lines mark the azimuth displacement of the blue starters in relative to the midway point of the two jet groupings. In the case here, they are ~10 km to the right of the midway point for these two blue starters.

[30] The optical strokes preceded these blue starters have relatively wide lateral spread compared with optical strokes occurred 0.5 s later at other locations. Since the orientation of the leader channel of the intercloud or intracloud lightning (ICs) is predominantly horizontal [*Rakov and Uman*, 2003, p. 327]; therefore, compared with CGs, the IC discharges are expected to produce wider horizontal spread on images. Admittedly, wide illuminations can still be produce by strong CG lightning. Without usable sferics data, the type of the causative lightning that produced these optical strokes cannot be distinguished. Simulation that was performed by *Riousset et al.* [2010] using a fix charging current to generate three ICs per minute indicates that the charge at the screen layer increases with the simulation time. With the occurrence of a −CG, negative charge are removed from the main charge layer in thundercloud. Hence the electric field at the upper part of the cloud increases creating a condition that favors the occurrence of blue jets/starters, whereas ICs would deplete the upper positive charge and thus reduce the electric field between the upper positive and the screen charge layers and impede the occurrence of the jets. Therefore it is more likely that the preceding optical strokes are due to −CG lightning. Under this scenario, the preceding −CGs increase the electric field in the upper region of the cloud and trigger the occurrence of the positive polarity jets. With the occurrence of these jets, the electric potential energy of the thundercloud was reduced and the lightning activity pauses until the cloud is charged up again. Figure 6b indicates that the optical strokes (lightning activity) near

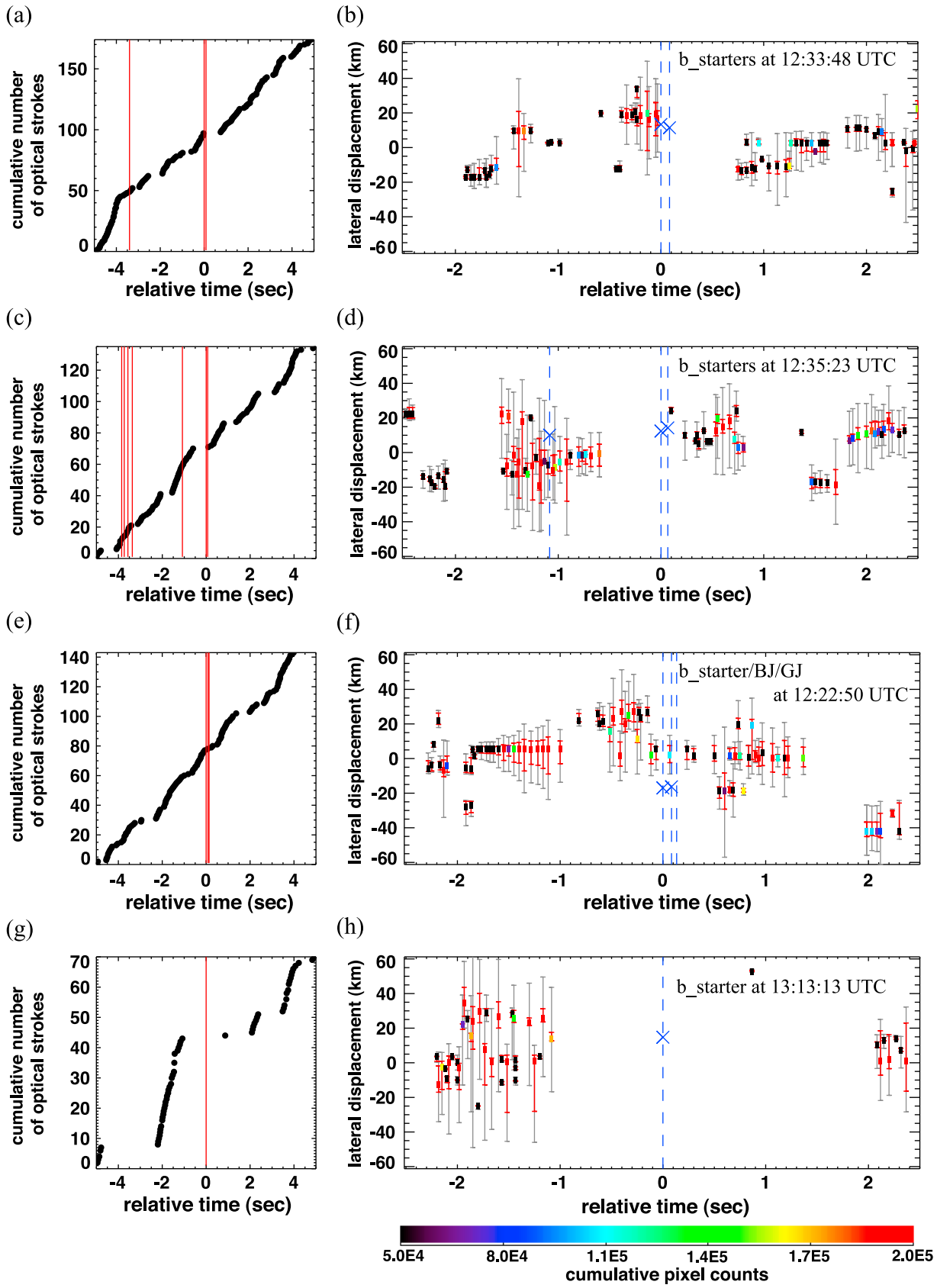
(a)
(b)
(c)
(d)
(e)
(f)
(g)
(h)
cumulative number of optical strokes
lateral displacement (km)
relative time (sec)
b_starters at 12:33:48 UTC
b_starters at 12:35:23 UTC
b_starter/BJ/GJ
at 12:22:50 UTC
b_starter at 13:13:13 UTC
5.0E4
8.0E4
1.1E5
1.4E5
1.7E5
2.0E5
cumulative pixel counts

Figure 6

the blue starters do not resume until ~1.8 s after the occurrence of these two blue starters.

[31] 2. Lightning activity pauses before the jets but increases after (9 events). As shown in Figure 6c, no optical stroke occurs within 0.5 s prior to the blue starters but the optical strokes appear frequently within 1 s following the blue starters. Figure 6d indicates that the trailing optical strokes occurred roughly at the location of the blue starters. Moreover, the optical strokes occurred before the blue starters appear to be nearby lightning. In the silent period before the blue starters, the cloud may have been charged continuously. The charging increases the upper positive charge and induces the screen charge to accumulate further as well. When sufficient charges are accumulated to enhance the electric field between these two layers beyond the breakdown threshold, a jet occurs readily. The ensuing optical strokes can be ICs or CGs. The modeling by *Riousset et al.* [2010, Figure 4a] points out that the lightning after the occurrence of blue jets are regular ICs due to the charging current from convection. However, it cannot be ruled out that the ensuing follow-up optical strokes are −CGs due to the occurrence of the preceding blue starters. In a region with strong charging current, the lower positive layer can be charged up. With the occurrence of blue jets from the upper charge layer that removed some upper positive charge, the electric field between main negative charge region and the lower positive charge layer can suddenly become very intense and favors the occurrence of −CG lightning. However, the current observation data are unable to resolve the nature of follow-up lightning.

[32] 3. Jets induced by nearby lightning activity (15 events). Figure 6e indicates that optical strokes flank prior and subsequent to this blue starter-blue jet-gigantic jet sequence, which was depicted in Figure 3. Figure 6f points out that the lateral displacements between the jets and the centers of the optical strokes are about 20 km. Clearly, the jets located outside the luminous range of the prior and subsequent optical strokes. Also, the polarity of the type II gigantic jet in this upward discharge event is believed to be positive cloud-to-ionosphere (+CI) [*Chou et al.*, 2010]. For this sequence of jets to happen, the main negative charge region beneath the jets may have been gradually drained by the nearby intracloud or intercloud lightning discharges (ICs) or negative cloud-to-ground discharges (−CGs) to a point that the electric field between the upper positive charge region and the screen charge layer exceeds the breakdown threshold. Figure 6f indicates that local optical strokes resume ~0.4 s after the jet sequence. It should be noted that there are four cases in this category with the blue jets/starters which locate near the edge of the FWHM azimuth span of the prior and subsequent optical strokes. However, these four blue jets/starters still could have been influenced by local or nearby lightning discharges.

[33] 4. No lightning activity both before and after the jet (1 event). This case occurred at 13:13:13 UTC, which is in the decaying phase of the jet-producing thunderstorm (Figures 2c, 6g, and 6h). The lightning activity is sporadic for this thunderstorm at this stage. There is no discernible optical stroke in the window 1 s before and 2 s after the occurrence of this blue starter. It is possible that very weak lightning discharges or deeply embedded discharges, whose optical emissions were either too weak or little have leaked out and thus eluded the detection of the low-light level CCD cameras, have helped to trigger this blue jet. Hence this case is similar to the −BJ reported by *Krehbiel et al.* [2008, Figure 2], which occurred in a decaying storm that had an inverted electrical structure. Using VHF mapping system, they detected an upward discharge in the unbalanced region caused by a preceding intracloud discharge occurring 10 s before. Furthermore, from the simulations reported in the supplementary information of *Krehbiel et al.* [2008] and by *Riousset et al.* [2010], the occurrence of +BJ shows a time delay in relative to the precursor −CG because the electric field is not immediately exceeding the breakdown threshold. So additional charging is required for the electric field to increase over the threshold. The charging current may have been low in this decaying storm, and the needed charging time thus is relatively long, which, in turn, caused this blue starter to appear as a standalone upward discharge.

[34] However, it should be noted that the above scenarios were inferred using optical data; the possibility of random collections of lightning and jets could not be excluded. Therefore further observations and studies with sufficient lightning data to confirm these inferred scenarios are needed.

7. Conclusions

[35] This paper reports the optical emissions and behaviors of 38 jets (37 blue jets/starters and 1 gigantic jet) observed over a thunderstorm in Fujian province of China, from the Lulin Observatory in Taiwan on 22 July 2007. Among these events, a short burst of 33 blue jets/starters occur in a 5 min window around 12:35 UTC, during the mature phase of this thunderstorm. Furthermore, a jet sequence begins with a blue starter, about 100 ms after a blue jet occurs at the same cloud top and then develops into a gigantic jet ~50 ms later. This is

Figure 6. (left) Representative cumulative patterns for optical strokes occurring within 50 km lateral distance and within a 10 s window of the observed jets. The red vertical lines mark the relative time of the jets. (right) Lateral span (gray lines), FWHM span (red lines), center (dots), and brightness (color of the dots) of the optical strokes within a 5 s window of the jets depicted on the left. Definitions of these quantities are given in section 5. The vertical blue dashed lines denote the relative occurrence times of the jets, and the crosses on the dashed lines mark the lateral distances of the jets relative to the midway point of the two jet groups; positive values mean to the right, and negatives mean to the left. (a and b) A blue starter–blue starter sequence at 12:33:48 UTC; lightning activity intensifies before the occurrence of the jets, while it is silent momentarily after. (c and d) A blue starter–blue starter sequence at 12:35:23 UTC; lightning activity pauses temporarily before the occurrence of the blue jets but intensifies after. (e and f) A blue starter–blue jet–type II gigantic jet sequence at 12:22:50 UTC; lightning activity increases both before and after the jets. (g and h) A lone blue starter at 13:13:13 UTC; no lightning activity occurs before or after the jet. The color palette denotes the cumulative pixel counts for the center column of an optical stroke.

the first type II GJ ever been observed from the ground. The preceding blue jet appears to act as the leading-jet-like discharge for the following gigantic jet; hence to some degree, the preceding blue jet behaviors similarly to the leading jet of the type I GJs recorded by *Su et al.* [2003]. In addition, a trailing-jet-like luminous column of this GJ rose up to ~35 km and lasted for ~17 ms. Therefore after completing the discharge channel to the ionosphere, the continuous current from the cloud top is less for the type II GJs compared with that in the type I GJs. Since the luminous emission of the trailing-jet-like column persists only for a short time, it is a good indication that the charge reservoir for this type II GJ was the upper charge layer and it had insufficient charge to supply a long-persisting trailing jet. This also implies that the type II GJ could be the blue-jet-type discharge discussed by *Krehbiel et al.* [2008].

[36] The jets reported in this work were recorded by a cluster of NTSC cameras, including a red band camera (passing band: 540–1000 nm) and a blue band camera (passing band: 340–540 nm). The jets exhibited significant red emissions in the images recorded by the red band camera. However, due to strong atmosphere scattering, the blue emissions from these jets were not discernible. A streamer emission model was used to estimate the emissions from blue starters and blue jets. Even though the quenching height of $1PN_2$ (red emissions) is ~53 km, owing to an exceptional broad passing band of the red band camera deployed in this observation, the red $1PN_2$ emissions from blue starters and blue jets are both detected.

[37] By analyzing the optical strokes on the recorded image frames, lightning activity near these jets was studied. Four representative correlation patterns between jets and lightning are found. One correlation pattern (pattern 1), which is similar to that reported by *Wescott et al.* [1996, 1998], indicates that lightning activity near the jets increased before the jets occur but fell silent subsequently for a short period of time. The jets were within the FWHM span of preceding optical strokes; hence the occurrence of these jets are likely to have been influenced by preceding local lightning. Assuming that the parent thundercloud having a normally electrified structure, the most probable scenario of the pattern 1 is the preceding local −CG lightning reduces the central negative charge causing the electric field in the upper cloud to exceed the breakdown threshold and trigger the jet to occur; with the occurrence of the jet, the electric potential of the cloud is reduced and instigate the lightning activity to stop for a while before resuming. The pattern 2 (lightning pauses before the jets but increases after) reveals that the occurrence of jets might affect the ensuing lightning activity near the jets. In pattern 3 (jets induced by nearby lightning), the jets appear to be induced by nearby IC or CG lightning discharges. While in pattern 4 (a standalone blue starter), this event occurred during the decaying phase of a thunderstorm, similar to the occurrence of a −BJ reported by *Krehbiel et al.* [2008, Figure 2]. The charging current may have been low in this decaying storm. Therefore a long duration is needed for the cloud to charge up before the jet can occur, and it makes this blue starter to appear as a standalone upward discharge. The first three correlation patterns provide evidence that supports the existence of interaction between upward discharging jets and the conventional cloud lightning.

[38] **Acknowledgments.** We are grateful to S. A. Cummer for helpful discussions and comments. We thank M. Sato for supplying the ELF data, Robert Holzworth for the WWLLN data, and P. H. Lin for comments on meteorology. Thanks to the staff at the Lulin observatory, Graduate Institute of Astronomy, National Central University, and to the staff at Central Weather Bureau in Taiwan for providing the radar reflectivity data and the infrared cloud map. Thanks also to Y. C. Chen, C. P. Hu, C. P. Wang, and Y. H. Lin for assistance. Work performed at NCKU was supported in part by NSPO and NSC in Taiwan under grants NSPO-S-100010, NSC99-2112-M-006-006-MY3, NSC97-2111-M-006-001-MY3, NSC99-2111-M-006-001-MY3, and NSC97-2111-M-006-004-MY3. The authors also would like to express their great appreciation to the two reviewers for their helpful and insightful comments.

[39] Robert Lysak thanks Jeremy Riousset and another reviewer for their assistance in evaluating this paper.

References

Amburn, S. A., and P. L. Wolf (1997), VIL density as a hail indicator, *Weather Forecasting*, *12*, 473–478, doi:10.1175/1520-0434(1997)012<0473:VDAAHI>2.0.CO;2.

Chou, J. K., et al. (2010), Gigantic jets with negative and positive polarity streamers, *J. Geophys. Res.*, *115*, A00E45, doi:10.1029/2009JA014831.

Cummer, S. A., J. Li, F. Han, G. Lu, N. Jaugey, W. A. Lyons, and T. E. Nelson (2009), Quantification of the troposphere-to-ionosphere charge transfer in a gigantic jet, *Nat. Geosci.*, *2*, 617–620, doi:10.1038/ngeo607.

Hsu, R. R., H. T. Su, A. B. Chen, L. C. Lee, M. Asfur, C. Price, and Y. Yair (2003), Transient luminous events in the vicinity of Taiwan, *J. Atmos. Sol. Terr. Phys.*, *65*, 561–566, doi:10.1016/S1364-6826(02)00320-6.

Knupp, K. R., B. Geerts, and S. J. Goodman (1998), Analysis of a small, vigorous mesoscale convective system. Part I: Formation, radar echo structure, and lightning behavior, *Mon. Weather Rev.*, *126*, 1812–1836, doi:10.1175/1520-0493(1998)126<1812:AOASVM>2.0.CO;2.

Krehbiel, P. R., J. A. Riousset, V. P. Pasko, R. J. Thomas, W. Rison, M. A. Stanley, and H. E. Edens (2008), Upward electrical discharges from thunderstorms, *Nat. Geosci.*, *1*, 233–237, doi:10.1038/ngeo162.

Kuo, C.-L. (2007), Analysis of sprites and elves recorded by the ISUAL scientific payload of FORMOSAT-2 satellite, Ph.D. thesis, Natl. Cheng Kung Univ., Tainan, Taiwan.

Kuo, C.-L., R. R. Hsu, A. B. Chen, H. T. Su, L. C. Lee, S. B. Mende, H. U. Frey, H. Fukunishi, and Y. Takahashi (2005), Electric fields and electron energies inferred from the ISUAL recorded sprites, *Geophys. Res. Lett.*, *32*, L19103, doi:10.1029/2005GL023389.

Kuo, C. L., A. B. Chen, J. K. Chou, L. Y. Tsai, R. R. Hsu, H. T. Su, H. U. Frey, S. B. Mende, Y. Takahashi, and L. C. Lee (2008), Radiative emission and energy deposition in transient luminous events, *J. Phys. D Appl. Phys.*, *41*, 234014, doi:10.1088/0022-3727/41/23/234014.

Kuo, C.-L., et al. (2009), Discharge processes, electric field, and electron energy in ISUAL-recorded gigantic jets, *J. Geophys. Res.*, *114*, A04314, doi:10.1029/2008JA013791.

Lang, T. J., W. A. Lyons, S. A. Rutledge, J. D. Meyer, D. R. MacGorman, and S. A. Cummer (2010), Transient luminous events above two mesoscale convective systems: Storm structure and evolution, *J. Geophys. Res.*, *115*, A00E22, doi:10.1029/2009JA014500.

Lyons, W. A. (1996), Sprite observations above the U.S. High Plains in relation to their parent thunderstorm systems, *J. Geophys. Res.*, *101*, 29,641–29,652, doi:10.1029/96JD01866.

Lyons, W. A., T. E. Nelson, R. A. Armstrong, V. P. Pasko, and M. A. Stanley (2003), Upward electrical discharges from thunderstorm tops, *Bull. Am. Meteorol. Soc.*, *84*(4), 445–454, doi:10.1175/BAMS-84-4-445.

Ontar Corporation (2002), PcModWin manual version 4.0, North Andover, Mass.

Pasko, V. P. (2003), Atmospheric physics: Electric jets, *Nature*, *423*, 927–929, doi:10.1038/423927a.

Pasko, V. P. (2010), Recent advances in theory of transient luminous events, *J. Geophys. Res.*, *115*, A00E35, doi:10.1029/2009JA014860.

Pasko, V. P., and J. J. George (2002), Three-dimensional modeling of blue jets and blue starters, *J. Geophys. Res.*, *107*(A12), 1458, doi:10.1029/2002JA009473.

Pasko, V. P., U. S. Inan, and T. F. Bell (1996), Blue jets produced by quasi-electrostatic pre-discharge thundercloud fields, *Geophys. Res. Lett.*, *23*, 301–304, doi:10.1029/96GL00149.

Pasko, V. P., M. A. Stanley, J. D. Mathews, U. S. Inan, and T. G. Wood (2002), Electrical discharge from a thundercloud top to the lower ionosphere, *Nature*, *416*, 152–154, doi:10.1038/416152a.

Petrov, N. I., and G. N. Petrova (1999), Physical mechanisms for the development of lightning discharges between a thundercloud and the ionosphere, *Tech. Phys.*, *44*, 472–475, doi:10.1134/1.1259327.

Raizer, Y. P., G. M. Milikh, and M. N. Shneider (2006), On the mechanism of blue jet formation and propagation, *Geophys. Res. Lett.*, *33*, L23801, doi:10.1029/2006GL027697.

Raizer, Y. P., G. M. Milikh, and M. N. Shneider (2007), Leader streamers nature of blue jets, *J. Atmos. Sol. Terr. Phys.*, *69*, 925–938, doi:10.1016/j.jastp.2007.02.007.

Rakov, V. A., and M. A. Uman (2003), *Lightning: Physics and Effects*, 850 pp., Cambridge Univ. Press, Cambridge, U. K.

Riousset, J. A., V. P. Pasko, P. R. Krehbiel, W. Rison, and M. A. Stanley (2010), Modeling of thundercloud screening charges: Implications for blue and gigantic jets, *J. Geophys. Res.*, *115*, A00E10, doi:10.1029/2009JA014286.

Rodger, C. J., S. Werner, J. B. Brundell, E. H. Lay, N. R. Thomson, R. H. Holzworth, and R. L. Dowden (2006), Detection efficiency of the VLF World-Wide Lightning Location Network (WWLLN): Initial case study, *Ann. Geophys.*, *24*, 3197–3214, doi:10.5194/angeo-24-3197-2006.

Sato, M., and H. Fukunishi (2003), Global sprite occurrence locations and rates derived from triangulation of transient Schumann resonance events, *Geophys. Res. Lett.*, *30*(16), 1859, doi:10.1029/2003GL017291.

Stolzenburg, M., T. C. Marshall, W. D. Rust, and B. F. Smull (1994), Horizontal distribution of electrical and meteorological conditions across the stratiform region of a mesoscale convective system, *Mon. Weather Rev.*, *122*, 1777–1797, doi:10.1175/1520-0493(1994)122<1777:HDOEAM>2.0.CO;2.

Su, H. T., R. R. Hsu, A. B. Chen, Y. C. Wang, W. S. Hsiao, W. C. Lai, L. C. Lee, M. Sato, and H. Fukunishi (2003), Gigantic jets between a thundercloud and the ionosphere, *Nature*, *423*, 974–976, doi:10.1038/nature01759.

Vallance-Jones, A. (1974), *Aurora*, D. Reidel, Norwell, Mass.

van der Velde, O. A., W. A. Lyons, T. E. Nelson, S. A. Cummer, J. Li, and J. Bunnell (2007), Analysis of the first gigantic jet recorded over continental North America, *J. Geophys. Res.*, *112*, D20104, doi:10.1029/2007JD008575.

Wescott, E. M., D. Sentman, D. Osborne, D. Hampton, and M. Heavner (1995), Preliminary results from the Sprites94 aircraft campaign: 2. Blue jets, *Geophys. Res. Lett.*, *22*, 1209–1212, doi:10.1029/95GL00582.

Wescott, E. M., D. D. Sentman, M. J. Heavner, D. L. Hampton, D. L. Osborne, and O. H. Vaughan (1996), Blue starters: Brief upward discharges from an intense Arkansas thunderstorm, *Geophys. Res. Lett.*, *23*, 2153–2156, doi:10.1029/96GL01969.

Wescott, E. M., D. D. Sentman, M. J. Heavner, D. L. Hampton, and O. H. Vaughan (1998), Blue jets: Their relationship to lightning and very large hailfall, and their physical mechanisms for their production, *J. Atmos. Sol. Terr. Phys.*, *60*, 713–724, doi:10.1016/S1364-6826(98)00018-2.

Wescott, E. M., D. D. Sentman, H. C. Stenbaek-Nielsen, P. Huet, M. J. Heavner, and D. R. Moudry (2001), New evidence for the brightness and ionization of blue starters and blue jets, *J. Geophys. Res.*, *106*, 21,549–21,554, doi:10.1029/2000JA000429.

Williams, E. R. (1998), The positive charge reservoir for sprite-producing lightning, *J. Atmos. Sol. Terr. Phys.*, *60*, 689–692, doi:10.1016/S1364-6826(98)00030-3.

P. L. Chang, Central Weather Bureau, Taipei 10048, Taiwan.

A. B. Chen, Institute of Space, Astrophysical and Plasma Sciences, National Cheng Kung University, Tainan 701, Taiwan.

C. M. Chen, J. K. Chou, R. R. Hsu, C. L. Kuo, Y. J. Lee, H. T. Su, and L. Y. Tsai, Department of Physics, National Cheng Kung University, Tainan 701, Taiwan. (rrhsu@phys.ncku.edu.tw)

L. C. Lee, Institute of Space Science, National Central University, Jhongli 32001, Taiwan.